Fuel 338 (2023) 127153

Contents lists available at ScienceDirect

Fuel

journal homepage: www.elsevier.com/locate/fuel

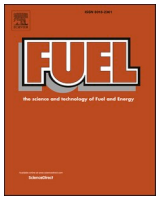

Full Length Article

Can diesel internal injector deposits form via an electrokinetic mechanism?

Radomir I. Slavchov [a], Ivan Radev [b], Wladimir Philippi [b], Volker Peinecke [b], Stuart M. Clarke [c,d], Sorin Filip [e]

[a] School of Engineering and Materials Science, Queen Mary University of London, Mile End Road, London E1 4NS, United Kingdom
[b] The Hydrogen and Fuel Cell Center GmbH, Carl-Benz-Strasse 201, D-47057 Duisburg, Germany
[c] Institute for Energy and Environmental Flows, University of Cambridge, Cambridge CB3 0EZ, United Kingdom
[d] Department of Chemistry, University of Cambridge, Cambridge CB3 0EZ, United Kingdom
[e] BP Formulated Products Technology, Research & Innovation, Technology Centre, Whitchurch Hill, Pangbourne, Berkshire, RG8 7QR, United Kingdom

ARTICLE INFO

Keywords:
Internal injector deposits
Deposition rate
Electrokinetic mechanism
Diesel
Autooxidation
Ion-radicals

ABSTRACT

A hypothetical electrokinetic mechanism of wear and deposition inside fuel injectors has been analysed theoretically and experimentally. It involves conjugated electrokinetic and earthing electric currents. The flow of fuel through the orifice of the injector produces a streaming current proportional to the ς-potential of the metal|fuel interface. The streaming current leads to an accumulation of streaming potential between the fuel in the combustion chamber and the fuel in the internal injector chambers. This potential drives an earthing current, which, at steady state, compensates the streaming current. The earthing requires electrochemical reactions to transfer charge through the metal|fuel interface of the internal parts of the injector. The hypothesis investigated here is that the reactions produce ion-radicals, which (i) initiate radical chains leading to oxidized deposit formation; (ii) produce fuel-insoluble electrolytic products. The hypothesis is tested experimentally using a rig where current is passed through two steel electrodes in fully formulated diesel at constant voltage. Accumulation of oxidation products (gum) in the diesel is observed with and without current, up to phase separation. The rate of deposition in the rig is found to be dominated by direct oxidative degradation rather than the electrokinetic mechanism.

1. Introduction

There is a class of hydraulic devices that all suffer from corrosion, accumulation of deposits, and wear that is unusual in that it occurs *upstream* of and onto the hydraulic control restrictions (orifices, valves). A common feature of these devices is a working fluid of low conductivity passing through a flow restriction. Three documented examples are:

(i) the orifice wear and film deposition in high-pressure servo valves and test rigs upon passage of hydraulic fluid [1–3];
(ii) the orifice wear [4,5] and the internal deposits [5–10] in diesel fuel injectors;
(iii) the deposits accumulating in the injecting device of the flow electrification test rig of Klinkenberg and van der Minne [11,12].

Journal and roller bearings also tend to suffer from wear upstream of a flow restriction [13]. Water-based systems, too, produce deposits and corrosion before flow restrictions – two well-studied cases are the so-called CRUD deposits in nuclear reactors [14,15] and the oxide deposition in models of boilers in advanced gas reactors [16].

The problems that these devices have been reported to experience are similar: pitting erosion and film deposition on the internal metallic surfaces. There is also a similar pattern in the flows of the respective working fluids and the conjugated electrokinetic and earthing electric currents in these devices, namely:

(i) the liquid flows through a restriction from an upstream container to a downstream container;
(ii) the migration of current upstream of the orifice through the liquid is partially or completely suppressed by a break in the conductive path (i.e. high electric resistance disallowing migration current through the fluid in the restriction);
(iii) the downstream and the upstream container are earthed.

The variations in three specific systems are summarized in Table 1; the pattern is schematically illustrated in Fig. 1.

The mechanism by which the metal surface is worn away upstream of the restriction in the case of phosphate ester hydraulic fluid has been

E-mail addresses: r.slavchov@qmul.ac.uk (R.I. Slavchov), i.radev@zbt.de (I. Radev).

https://doi.org/10.1016/j.fuel.2022.127153
Received 9 July 2022; Accepted 11 December 2022
Available online 2 January 2023

investigated in detail by Beck et al. [1,2,3,13,17]. The motivation for their research was the wear occurring in aircraft slide and sleeve hydraulic servo valves, upstream of and just within the orifice, in the form of small pits eventually covering the entire surface. Beck et al. showed that the turbulent flow through the orifice causes a significant streaming current, I_s, proportional to the electrokinetic ς–potential of the orifice surface ($\varsigma \sim 200$ mV [2], an order of magnitude typical for metals in contact with fluid of low conductivity [11]). The conductivity of the hydraulic liquid ($\sim 10^{-5}$ Ω^{-1}cm^{-1}) is too low to compensate for the resulting accumulation of charge and streaming potential; the orifice mitigates the reverse migration current, acting as a break in the circuit. As a result, the streaming potential, ϕ_s, increases to values high enough to induce electrochemical reactions at the interface metal|phosphate ester and a respective earthing current I_e. The observed wear is the result of the electrochemical corrosion produced by currents through the interface. Beck et al. [1] built an electrode system to measure the actual I_e passing from an electrode downstream of the orifice to an electrode upstream and obtained values consistent with those they computed via an elegant model they developed. They also showed directly that the electrochemical reaction at the anode involves dissolution of the metal [17]. Further, they combined Faraday's law with their model to compute the wear profile produced by I_e, which agreed reasonably well with the one obtained in a specially designed test rig [1]. Finally, Beck et al. undertook tests (application of external voltage; changing the material in the corrosion zone) to show that other wear mechanisms (cavitation, abrasion) are not consistent with their observations. The mechanism helped them to formulate additive packages containing an anti-erosion component designed to mitigate the streaming current, and the resultant electrochemical corrosion [3].

Even earlier than Beck et al., Davies and Rideal [12] proposed the same mechanism as a qualitative explanation for the accumulation of deposits in the oil container upstream of the restriction in the electrification test rig of Klinkenberg and van der Minne. Davies and Rideal realized that the streaming current in this apparatus has to be compensated by a current passing between earth and the liquid in the upstream container, which results in the accumulation of insoluble products of electrolysis (as the metal is unlikely to dissolve in the oil phase the way it does in the phosphate ester in Ref. [17]). Davies and Rideal did not seek further description of the process. The possibility for the earthing current to cause deposits instead of wear was also demonstrated by Beck et al. [1,17], who observed in various geometries a deposited film at the cathode, and also at the anode far away from the orifice (i.e. at lower anodic potentials). The same corrosion mechanism has been rediscovered for the third time by Varga and Dunne, with flow of ultra-pure water through valves [18], and for a fourth time by Touchard, Romat, Chen and Radke [19,20] for an alkane flowing through a metal capillary.

The first goal in the present work is to investigate the possibility that electrokinetic-induced corrosion causes wear and deposit accumulation inside fuel injectors; to use a modification of the model of Beck et al. to give some bounds to the rate of the wear/deposition process; and to investigate theoretically some possible reaction routes and products (Section 2).

The second goal is to investigate the hypothesis of Beck et al. [17] that sludge formation in oils can be induced by a related electrokinetic mechanism. By "sludge" we refer to the product of low-temperature (<200 °C) oxidation of organic components of the oil and the fuel. The accumulation of oxidation products in the internal lines of diesel injectors has indeed been reported, especially for diesels with FAME-blend [10,21,22]. An ever-present problem with all autooxidation processes in hydrocarbons is the identification of the source of radicals that initiate the radical chains leading to fuel degradation [23,24]. It is significant that there is no obvious major source of radicals in the fuel line. Here we propose a mechanism for the production of radicals by the earthing currents in Section 2, as an extension of the theory of Beck et al. We show that, when applied to a high-pressure injector nozzle orifice and fuel of low conductivity, a new regime of flow and current streaming can be expected (perfect filtration of the coions). In addition, we develop a model of the deposition, including electrolyte precipitation and initiation of a radical chain autooxidation. Section 3 is dedicated to the experimental test of this hypothesis.

2. Hypothesis

Mechanism. Consider an injector spraying fuel into a cylinder. The upstream container is the internal injector fuel line; the downstream container is the combustion cylinder; the restriction is the nozzle orifices (Fig. 1a). The spray acts as an insulating element because the continuous gas phase is of negligible conductivity. For definiteness, we will assume that the ς-potential of the nozzle orifice|fuel interface is positive, and that the fuel spray impinges on the piston surface. The mechanism of Beck et al., as applied to fuel injection, involves the following steps:

(i) the fuel jet injected through the nozzle holes carries a streaming current I_s. The nozzle orifices, with their positive ς-potential, act as a filter for the positive ions (which remain trapped in the internal fuel line), while the spray transports the negative ions to the cylinder.

(ii) The streaming current I_s results in the accumulation of a streaming potential difference, $\phi_s < 0$, between the cylinder (where negative charge accumulates) and the fuel line (where the cations are trapped). Initially, each injection produces an increase in the absolute value of ϕ_s.

(iii) According to Tafel's equation, as ϕ_s increases, so do the rates of the electrochemical reactions at the metal|fuel interfaces at the anode (the spray impingement zone) and the cathode (the injector internal line). These electrochemical processes result in electron transfer through the two phases and an earthing current I_e normal to the steel walls. After a certain number of injections, I_e and ϕ_s reach steady state values, corresponding to the balance

Table 1
Comparison between hydraulic devices suffering from deposits and wear.

hydraulic device	hydraulic servo valves and a respective test rig [1–3]	diesel fuel common rail injector	flow electrification test rig [11,12]
low-conductivity fluid	hydraulic fluid with phosphate ester base	diesel fuel	white oil, non–additized and additized fuels, hydrocarbons
restriction	slit orifice	injector nozzle orifices	injecting metal capillary
upstream container	upstream chamber	fuel line (needle chamber)	a metal container (earthed to the trough)
downstream container	downstream chamber	combustion cylinder	an insulated trough
liquid conductivity line cut	ensured by the small cross-section of the orifice and the low conductivity of the fluid; cut not perfect – some back-current through the liquid still occurs [1]	ensured by the breakage of the high-momentum spray into fine droplets; cut nearly perfect	low conductivity of the liquid combined with large distance between the capillary and the trough; the liquid jet breaks after a critical distance; cut not perfect – some back-current through the liquid occurs [2,11]
observed wear and deposits	erosion of the orifice entrance, formation of a deposit film further away	deposits or/and wear at the needle seat, ball, nozzle orifice [4–10]	deposits in the capillary and in the metal container

$$I_e(\phi_s) = -I_s \quad (1)$$

In order to explain the appearance of autooxidation products – gum and sludge – in the fuel, the mechanism of Beck et al. has to be extended by postulating two additional steps:

(iv) the electrochemical reaction involves a *'weak' fuel component* prone to oxidation–reduction reactions, F, which produces *ion-radicals* upon reduction or oxidation at relatively low ϕ_s.
(v) Each ion-radical initiates an oxidative radical chain, producing several oxidized molecules per ion.

There are many variations of this mechanism. Three scenarios can be mentioned that are equally probable as the one postulated above.

(var1) We have assumed a positive ς-potential, which could be either due the chemistry of the steel surface or due to specific adsorption of positively charged components of the fuel – e.g., the anti–static agent $Ca^{2+}(diisopropylsalycilate^-)_2$ causes charging via the positive $[Ca^{2+}(diisopropylsalycilate^-)]$ ion [11]. Alternatively, the ς-potential of the metal|diesel interface can be negative, e.g., due to carboxylate ions adsorbing from the fuel to the steel; in this case, the anode will be located in the internal injector fuel line, while the piston surface will serve as the cathode.

(var2) If the spray does not impinge on the piston surface, then the charge streamed into the cylinder will be discharged elsewhere – on the cylinder walls (the liner, the head), the exhaust valve, and downstream in the exhaust system. Changing the location will change the conditions at the anode without affecting the cathode.

(var3) The balance of currents can be complicated by two other currents countering I_s. The first is charge transport via sparks [25,26]; this option has to be avoided in engines, and this is the reason why the injectors and the cylinder components are carefully earthed in the first place. Nevertheless, sparks can be expected in the case where a growing deposit film insulates [11] the cathode. The second possibility is a migration current upstream of the spray (considered by Beck et al. and others [1,2,11]), which, in the case of fuel sprays, requires conductivity of the gas phase.

It should be stressed that the fuel injection process is discontinuous. Each engine cycle continues for time of the order of 50 ms. The nozzle orifices remain opened for a shorter period (0.1–1 ms), and once they close, the fuel in the internal line has some time to redistribute the trapped excess positive charge.

Let us now consider the quantitative aspects of this mechanism.

Streaming current. The turbulent electrokinetic current I_s carried by hydrocarbons and fuels flowing through narrow channels has been investigated in some detail in relation to the electrification phenomenon that caused many accidents in the oil industry [11]. The theory of the phenomenon has been developed for a range of conditions and flow geometries [11,27–29] (cf. Ref. [30] for a concise review). Yet, the simple Bernoulli flow through a short cylindrical orifice is among the least studied cases; therefore, some assumptions have to be made to

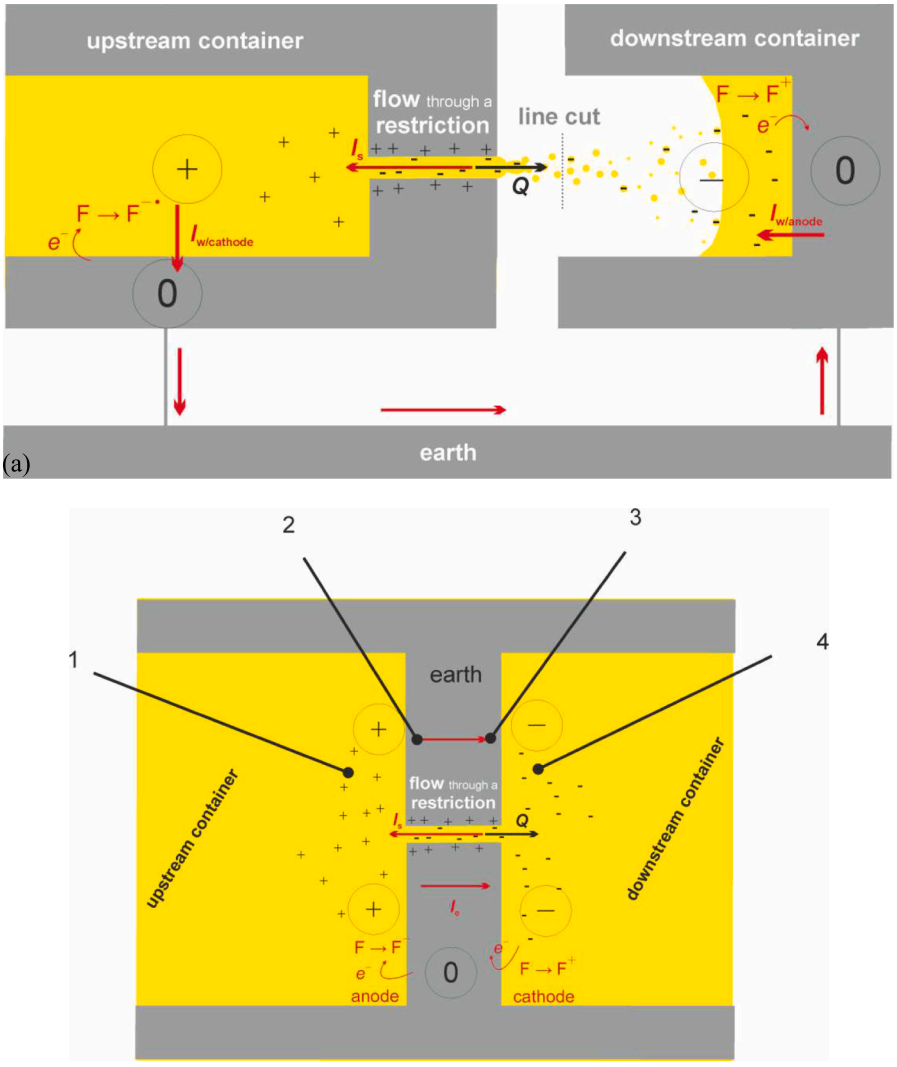

Fig. 1. General pattern of the flow and proposed mechanism leading to the wear and deposition. (a) Injector nozzle geometry. (b) Orifice geometry. In both cases, the streaming current I_s (driven by the liquid discharge Q through the restriction) leads to the accumulation of a potential difference on the two sides of the restriction (potential signs compared to earth's 0 indicated in circles). This potential accumulates until the charge transfer through the walls (i.e. the cathodic and the anodic reactions $F \rightarrow F^{\pm} \pm e^-$, where F is a reactive fuel component) accelerates enough to compensate I_s via the earthing current I_e through the metal.

estimate I_s.

Most modern nozzle orifices are of small radii ($R_n \sim 50$–100 μm). At the same time, the fuels are characterized by large Debye lengths (i.e. thick electric double layers at the steel|fuel interface). The Debye length L_D in electrolyte solution containing positive and negative monovalent ions of concentration C_e is given by

$$L_D = \sqrt{\frac{\varepsilon k_B T}{2e^2 C_e}} = \sqrt{\frac{\varepsilon D}{\kappa}} \tag{2}$$

here, ε is the absolute dielectric permittivity of the fuel; e is elementary charge; k_B is the Boltzmann constant; T is the temperature; we used the relationship $\kappa = 2e^2 D C_e / k_B T$ between conductivity κ and the mean diffusion coefficient D [31]. In oils, the usual Debye-Hückel formula $L_D \propto C_e^{-1/2}$ is of little use, as C_e is difficult to estimate due to the significant degree of association of the electrolytes in such low-dielectric-constant media. In contrast, ε and κ are known and D can be estimated [11].

A typical hydrocarbon has specific conductivity of the order of 10^{-12} $\Omega^{-1}m^{-1}$. Diesel fuels always contain impurities, and anti-static and other electrolytic additives that increase κ to (50–500) $\times$ 10^{-12} $\Omega^{-1}m^{-1}$ at room temperature, to comply with diesel regulations [32,33]. Furthermore, the conductivity increases significantly for hot fuel. At the injector operating temperature (70–130 °C in the main fuel line), using van't Hoff's dependence and the value 20 kJ/mol for the heat of dissociation of the electrolyte [33], one can expect $\kappa = (200\text{–}2000) \times 10^{-12}$ $\Omega^{-1}m^{-1}$. The order of magnitude of the diffusion coefficient of dodecanol in water is 5×10^{-10} m^2/s [34]; the organic ions in diesel can be assumed to be of similar Stokes radii. The viscosity of diesel at 70–130 °C is a factor of 5 higher than that of water at 25 °C; hence, using the Stokes-Einstein relation, we obtain $D = 10^{-10}$ m^2/s. Finally, $\varepsilon = 2.2 \times \varepsilon_0$ [33]. From eq. (2), it then follows that the *static* Debye length in diesel is $L_D = 1$–3 μm. The relaxation time of the double layer is of the order of [11] $\tau = L_D^2/D \sim 10$–100 ms, much longer than the duration of the injection, meaning that the structure of the double layer will not be static during the injection. In addition, the Reynolds number Re for the flow through the orifice is high: using Bernoulli's law, for 2000 bar injection pressure, the fluid velocity is $v = 730$ m/s; for nozzle radius $R_n = 100$ μm and vena contracta radius [35] of 80 μm, $Re \sim 15000$. Under such conditions, the electric double layer protrudes inside the developed turbulent flow, and the convection due to the turbulent eddies is able to overcome the electrostatic forces to effectively mix the diffuse part of the double layer with the uncharged core of the flowing liquid, ideally producing a homogeneous charge distribution in the bulk. It has been argued that in this case the double layer extends to a characteristic *turbulent Debye length*, which can be estimated from the value of the so-called coefficient of eddy diffusivity D_{eddy} [11]:

$$D_{eddy} = 0.018 R_n \bar{v} Re^{-1/6} \tag{3}$$

D_{eddy} is 250 $\times$ 10^{-6} m^2/s for the above numbers, 4–5 orders of magnitude higher than the static D. As a result, the electric double layer extends to [11] $L_{D,eddy} \sim (D_{eddy}\tau)^{1/2} \sim 1$–$5$ mm, an order of magnitude larger than the nozzle diameter. This estimate allows us to use the simplifying assumption that the liquid flowing through the nozzle is well-mixed, and the charge it carries is homogeneous.

Accordingly, we consider two regimes of the streaming current. The first one corresponds to *turbulent electroneutral flow*, and holds at high Reynolds number, relatively low surface charge ρ_e^S, relatively high conductivity of the liquid, and large nozzle radii ($|\rho_e^S| < eC_eR_n/2$). It was realized by Rutgers et al. [27] that the charges in the liquid phase should be uniformly distributed in this case. The interface metal|oil is characterized by a high ς-potential but small surface charge density ρ_e^S (small number of specifically adsorbed ions). The relation between the two,

$$\rho_e^S = \varepsilon\varsigma / L_D \tag{4}$$

shows that when ε is small (low medium polarizability) and L_D is long (little screening), a very small surface charge (1 charge per 1×1 μm^2 for an alkane) is enough to produce potentials of the order of 100–500 mV. For comparison, in dilute aqueous electrolyte, surface charge has to be 4–5 orders of magnitude higher to produce the same potential. A stationary turbulent flow through a cylindrical tube will carry a bulk charge density ρ_e, related to ρ_e^S via the electroneutrality condition:

$$\pi R_n^2 \rho_e = -2\pi R_n \rho_e^S \tag{5}$$

The streaming current is simply the product of ρ_e and the volumetric flow rate Q:

$$I_s = \rho_e Q = -2\rho_e^S Q / R_n \tag{6}$$

In case that the flow does not alter ρ_e^S, one can use eq. (4) to express I_s through the standard "laminar" value ς of the electrokinetic potential and the static Debye length L_D:

$$I_s = -\frac{2\varepsilon\zeta}{L_D R_n} Q = -\frac{2\zeta}{R_n}\sqrt{\frac{\varepsilon\kappa}{D}} Q \tag{7}$$

The minus sign reflects the fact that the charge carried to the cylinder by the streaming current is opposite to the charge of the surface.

Eq. (6) has a wider range of validity than eq. (7), as the latter involves the assumption that ρ_e^S is independent of the flow rate and the size of the nozzle. Both assumptions are inaccurate – the cavitation phenomenon at high Re can alter the conditions at the surface, and when L_D is comparable with R_n, charge regulation can be expected to shift both the surface potential and the surface charge [20]. Eq. (7) can be compared with Smoluchowski's formula valid for laminar flow,

$$I_{s,laminar} = -8\varepsilon\zeta Q / R_n^2 \tag{8}$$

The ratio of the streaming currents in turbulent and in laminar regimes is $I_s/I_{s,laminar} = R_n/4L_D$, which is of the order of 10 (the same amount of liquid passing through the same orifice will carry through more charge if its flow is turbulent).

The second regime we consider ("*perfect filter*") is again at high Reynolds number, but at high surface charge, low conductivity of the liquid and small nozzle orifice radius. Eq. (5) will not hold true if $|\rho_e^S| > eC_eR_n/2$, as ρ_e cannot exceed eC_e under the assumption of good mixing. In this case, the negatively charged liquid inside the orifice is unable to neutralize the positive surface charge; as a result, the orifice shall act as a perfect filter for the co-ions – all available cations remain trapped upstream due to the high electrostatic barrier caused by the excess orifice charge, while all anions pass freely. This limit corresponds to a streaming current of

$$I_s = -eC_eQ = -\frac{k_B T \kappa}{2eD} Q \tag{9}$$

where we used the relation $C_e = k_B T\kappa / 2e^2 D$. The sign of I_s is minus since we assumed $\rho_e^S > 0$; it will be plus in the opposite case.

For diesel of relatively high conductivity (500 $\times$ 10^{-12} $\Omega^{-1}m^{-1}$), the streaming current is more likely to follow the electroneutral flow regime, and eq. (7) predicts I_s of the order of 1 μA for the injection duration (assuming $\varsigma = 200$ mV, corresponding to 1 adsorbed charge per 0.3×0.3 μm^2). For diesel of lower conductivity (50 $\times$ 10^{-12} $\Omega^{-1}m^{-1}$), the flow can be expected to be in a mixed regime (flow not electroneutral but the 'filter' will not be quite perfect for the cations). For this conductivity, both eq.(7) and (9) predict $I_s \sim 0.4$ μA. The fuel mass injected per cycle for a passenger car is typically 20 mg, corresponding to 0.7–2 nC of charge per injection, or, by dividing by the engine cycle duration, 15–50 nA average current for all 6 nozzles (for engine speed of 2800 rev/min), or average $\langle I_s \rangle = 3$–10 nA per nozzle.

There are several complications that have been neglected in the estimates above. The first is the edge effects – when the length of the nozzle orifice is comparable with its diameter, eq. (5) becomes inaccurate, giving a decrease in the absolute value of the charge carried by the spray. The second is that the strong image force acting nearby the metal

is likely to provoke dissociation of the salts in the channel and even in the internal fuel line (the presence of a conductor nearby stabilizes the ions) – hence, an increase of the conductivity and the streaming current can be expected.

Streaming potential. Whatever the regime, the streaming current accumulates negative charge in the cylinder and positive charge inside the injector, resulting in a respective streaming potential ϕ_s. To avoid the risk of sparks due to dangerously high ϕ_s, the injector and the piston are carefully earthed. The steady state charge of the fuel in the injector and the streaming potential are limited by the current passing between earth and fuel, which ideally maintains the fuel at earth potential in spite of the electrokinetic loss of anions. Actually, due to the low conductivity of the fuel, the characteristic time for earthing is significant and fuel upstream of the orifice remains at significantly more positive potential compared to earth [11].

The earthing current I_e is necessarily a surface reaction current – the electron transfer through the interface is the result of an electrochemical reaction. The products of this reaction are either dissolved in the fuel [1,3] or remain adsorbed at the steel|fuel interface [3,12]; this may involve dissolution of the metal in the upstream container [1,3] and its deposition downstream [20]. The detailed mechanism of the degradation process has never been the focus of investigation of the workers who studied the streaming currents carried by fuel, and little is known about it. Touchard, Radke et al. [19,20,36] investigated the case where the electrode is assumed to be of the first kind [37], i.e. the main electrochemical reaction is $M \leftrightarrow M^{n+} + ne^-$, where M is the electrode metal, and M^{n+} is a metal ion dissolved in the oil phase. As the free energy of an ion dissolved in oil is high, it is more likely that the electrode is instead of the second kind [37] (a salt $M^{n+}A_n^-$ of low solubility is formed at the surface of the electrode, where A^- is an ion present in the fuel, as assumed by Paillat et al. [36]), or alternatively the electrode is inert (a *redox system* [37]) and just provides/consumes the electrons of a reaction $F \leftrightarrow F^{\pm\cdot} \pm e^-$, where F is a fuel component prone to electron transfer.

The electrochemical degradation of organic molecules follows different pathways for different molecules, yet the mechanism often has two distinct steps:

(i) the species F prone to reduction or oxidation produces either one neutral radical and one ion or one ion-radical, by electron transfer through the metal.
(ii) The radical then initiates chain autooxidation reactions, producing oxygenates without further charge transfer.

The reactions at the cathode and the anode are, in principle, markedly different [3], and therefore, a change in the sign of the ζ-potential from positive to negative with a suitably chosen fuel component should be expected to change the nature of the corrosion products upstream of the nozzle.

Let us give a couple of examples for anodic and cathodic reactions of well-understood mechanisms which are possible at the interface steel|diesel. One example is the **anodic** Kolbe electrolysis of *carboxylic acids*; the first step of this reaction in a polar solvent is [38]:

$$R_FCH_2COO^- \rightarrow R_FCH_2\cdot + CO_2 + e^- \text{(anodic reaction)}, \tag{10}$$

where the reactivity of the acid is higher when R_F is phenyl, α-alkenyl or another substituent able to stabilize $R_FCH_2\cdot$. In the oil phase, the carboxylic ion is likely to be in an ionic couple with a counter-ion, which is released by the reaction. This counter-ion will either bind into a new ionic couple with the anions present in the fuel or will precipitate them. The fate of the radical $R_FCH_2\cdot$, in the fuel phase and in the presence of oxygen, is to initiate an autooxidation process [23]:

$$R_FCH_2\cdot + O_2 \rightarrow R_FCH_2O_2\cdot;$$

$$R_FCH_2O_2\cdot + RH \rightarrow R_FCH_2O_2H + R\cdot, \tag{11}$$

where $-O_2H$ is a hydroperoxy group and RH can be any fuel component having a weak C—H bond (in particular, tertiary and secondary C—H at α-position with respect to a double bond, phenyl, >C═O or other polar groups [23]). The auto-oxidation chain is continued by R· until termination occurs:

$$R\cdot + O_2 \rightarrow RO_2\cdot;$$

$$RO_2\cdot + RH \rightarrow RO_2H + R\cdot;$$

$$2RO_2\cdot \rightarrow \text{termination products}. \tag{12}$$

Another family of relatively well-studied anodic reactions is the oxidation of *nitrocompounds*. For example, the first step of the Shono reaction mechanism [39,40] is:

$$R_{F1} - CO - NH - R_{F2} \rightarrow R_{F1} - CO - N^{+\cdot}H - R_{F2} + e^- \text{(anodic reaction)}. \tag{13}$$

In the presence of O_2 and in hydrocarbon medium, the next step of the Shono reaction will not follow the route they do in polar solvents. Instead, a standard radical chain is again likely:

$$R_{F1} - CO - N^{+\cdot}H - R_{F2} + RH \rightarrow R_{F1} - CO - N^{+}H_2 - R_{F2} + R\cdot, \tag{14}$$

and the outlined route thereafter. Most diesel fuels contain labile nitrocompounds – they are used as dispersants, cetane improvers and anti-static additives [41,42].

Finally, many *aromatic hydrocarbons* are prone to electrolytic oxidation, but the study of this process has been hindered by the fact that it produces solid carbonaceous deposits [43] that are difficult to analyse.

As a generalization, we assume that the cathodic reaction involves a fuel component F, most probably one of polar chemistry as this ensures both high adsorption activity and high reactivity. The general reaction pathway involves a cathodic reaction producing anion-radical, and a subsequent initiation reaction with a fuel component RH:

$$F + e^- \rightarrow F^{-\cdot}, \qquad \nu_e^S = |I_s|/e;$$

$$F^{-\cdot} + RH \rightarrow FH^- + R\cdot, \qquad \nu_i^S = k_i[F^{-\cdot}]^S[RH] \tag{15}$$

where ν_{es} and ν_i^S are the rates of the reactions, in units $[s^{-1}]$ and $[m^{-2}s^{-1}]$, respectively; the first equation is Faraday's law, and $[F^{-\cdot}]^S$ is the surface concentration of $F^{-\cdot}$. Similar processes occur at the anode, but with the formation of cation-radicals:

$$F \rightarrow F^{+\cdot} + e^-, \qquad \nu_e^S = |I_s|/e;$$

$$F^{+\cdot} + RH \rightarrow FH^+ + R\cdot, \qquad \nu_i^S = k_i[F^{+\cdot}]^S[RH]. \tag{16}$$

Of course, F and RH can be different at the cathode and the anode. The case where the anodic/cathodic reaction produces one ion and one radical instead of a single ion-radical differs little. Both mechanisms (15) & (16) produce alkyl R· (presumably tertiary alkyl, phenylalkyl or alkenylalkyl) that is oxidized following the well-known mechanism [23]:

$$R\cdot + O_2 \rightarrow RO_2\cdot, \qquad \nu_o = k_o[R\cdot][O_2];$$

$$RO_2\cdot + RH \rightarrow RO_2H + R\cdot, \qquad \nu_a = k_a[RO_2\cdot][RH];$$

$$2RO_2\cdot \rightarrow \text{terination products} + O_2, \qquad \nu_t = k_t[RO_2\cdot]^2. \tag{17}$$

The radicals $F^{-\cdot}$, R· and $RO_2\cdot$ are assumed to be reactive intermediates, so that the steady state approximation holds true:

$$d[F^{-\cdot}]\Big/dt = |I_s|\Big/e - \int \nu_i^S dA \approx 0, \quad \text{so} \quad \int \nu_i^S dA = |I_s|\Big/e; \tag{18}$$

$$Vd[R\cdot]\Big/dt = V\nu_a + \int \nu_i^S dA - V\nu_o \approx 0, \quad \text{so} \quad \nu_o = \nu_a + |I_s|\Big/Ve; \tag{19}$$

$$\mathrm{d}[\mathrm{RO_2}\cdot]/\mathrm{d}t = v_\mathrm{o} - v_\mathrm{a} - 2v_\mathrm{t} \approx 0, \quad \text{so} \quad 2v_\mathrm{t} = |I_\mathrm{s}|/Ve, \tag{20}$$

and similarly for the anode; the integration is over the area A of the metal|oil interface, and V is the volume of the fuel. Substituting eq. (17) into eq. (19) & (20) and solving for $[\mathrm{R}\cdot]$ and $[\mathrm{RO_2}\cdot]$, we obtain the stationary state concentrations of the radicals:

$$[\mathrm{RO_2}\cdot] = \sqrt{\frac{|I_\mathrm{s}|}{2k_\mathrm{t}Ve}}; \qquad [\mathrm{R}\cdot] = \frac{k_\mathrm{a}[\mathrm{RH}]}{k_\mathrm{o}[\mathrm{O_2}]}\sqrt{\frac{|I_\mathrm{s}|}{2k_\mathrm{t}Ve}} + \frac{|I_\mathrm{s}|}{k_\mathrm{o}[\mathrm{O_2}]Ve} \tag{21}$$

We further assume that the ions FH^- and FH^+ eventually recombine with the excess cations C^+ in the upstream container and with the excess anions A^- in the downstream container, respectively, to form insoluble salts at the surface:

$$\mathrm{FH}^- + \mathrm{C}^+ \rightarrow \mathrm{CFH}\downarrow; \qquad \mathrm{FH}^+ + \mathrm{A}^- \rightarrow \mathrm{FHA}\downarrow. \tag{22}$$

Paillat et al. [36] considered another variant of such "precipitation" reactions, with FH^+ being a metal ion. The rate of formation of insoluble salts at the cathode is given by

$$v_{\text{ionic deposit}} = V\mathrm{d}[\mathrm{FH}^-]\Big/\mathrm{d}t = \int v_\mathrm{i}^\mathrm{S}\mathrm{d}A = |I_\mathrm{s}|\Big/e, \tag{23}$$

and similarly for the anode; $v_{\text{ionic deposit}}$ is in units s^{-1}. Here, eq. (18) has been used. Thus, the amount of the produced electrolyte depends on the magnitude of the streaming current *only*. According to eq. (23), each excess charge passing through an injector orifice results in one charge crossing the metal|fuel interface and one precipitation event like (22) at each electrode.

Finally, for the rate of oxygen and fuel consumption by the oxidation chain, we obtain:

$$-\frac{\mathrm{d}[\mathrm{O_2}]}{\mathrm{d}t} = v_\mathrm{o} - v_\mathrm{t} = \left(\frac{1}{2} + \nu\right)\frac{|I_\mathrm{s}|}{Ve}$$

$$-\frac{\mathrm{d}[\mathrm{RH}]}{\mathrm{d}t} = v_\mathrm{a} + \frac{|I_\mathrm{s}|}{Ve} = (1+\nu)\frac{|I_\mathrm{s}|}{Ve} \tag{24}$$

here, we introduced *the radical chain length*, ν, which, by definition, is given by [23]:

$$\nu = \frac{Vv_\mathrm{a}}{\int v_\mathrm{i}^\mathrm{S}\mathrm{d}A} = k_\mathrm{a}\sqrt{\frac{Ve}{2k_\mathrm{t}|I_\mathrm{s}|}}[\mathrm{RH}] \tag{25}$$

where the second equation (17) has been used together with the expression (21) for $[\mathrm{RO_2}\cdot]$. The amount of the oxidation products produced per unit time is $-V\mathrm{d}[\mathrm{RH}]/\mathrm{d}t$. Therefore, the ratio of Eq. (23) and (24) is

$$\frac{\text{moles of products of oxidation}}{\text{moles of electrolytic products}} = -\frac{V}{v_{\text{ionic deposit}}}\frac{\mathrm{d}[\mathrm{RH}]}{\mathrm{d}t} = 1 + \nu, \tag{26}$$

i.e. for each molecule of precipitated electrolyte, one has $1 + \nu$ oxidized molecules produced in the oil. For 1-octene and ethylbenzene, $k_\mathrm{a}/(2k_\mathrm{t})^{1/2} = 1690 \times \exp(-41.1\ \mathrm{kJ/mol}/RT)\ \mathrm{s}^{-1/2}\mathrm{M}^{-1/2}$ and $251 \times \exp(-36.0\ \mathrm{kJ/mol}/RT)\ \mathrm{s}^{-1/2}\mathrm{M}^{-1/2}$, respectively (table 2.1 of Ref. [23]; these rates are for 2 reactive C—H bonds), or around 0.001–0.005 $\mathrm{s}^{-1/2}\mathrm{M}^{-1/2}$ at 80–120 °C. The concentration [RH] of alkenes and arenes in diesel is of the order of 1 M, and we assume that each has two labile C—H bonds on average. The volume affected (the chambers nearby the 6 nozzles) is of the order of 1 mm^3. For streaming current of 15–50 nA for all nozzles, we obtain ν = 2–15 (compared to ν = 1–50 for various auto-oxidation processes [23]).

It is noteworthy that the rate of formation of oxidation products is a function of I_s and ν only, but not of other factors such as oxygen concentration, or the nature of the molecule F that takes part in the electron transfer reaction, or the rate parameters k_o and k_i. This feature is typical for auto-oxidation reactions [23,44], but may not hold in cases where the oxygen concentration is below 1 mM, or the system is not in the steady state regime.

It is difficult to predict the fate of the oxidation products a priori. The primary products are peroxides. They can adsorb on the steel surface or remain dissolved and associate with other polar molecules in the bulk phase; they can oxidize further to ketones, acids and polymers [23] or decompose to alkoxy radicals and accelerate the auto-oxidation process (branching) [23,44]. Eventually, the oxidation degradation products can get deposited on the surface. Some of the peroxides may find their way back to the fuel tank through the control valve via the fuel return and accelerate fuel aging.

Chemistry of the deposits. The diverse chemistry reported for the internal injector deposits is in broad agreement with what follows from the mechanism described here. The internal injector deposits are a complex polydisperse system, containing carbonaceous decomposition products, organic amide lacquers, inorganic [6,45] and soapy organic electrolytes [6–9,21,46]; the aged deposits can be polyaromatic [6–9,47,48] and even graphitic. The chemistry of the anti-static additives is particularly similar to the electrolytic content in the internal injector deposits, which could be explained by ions of these additives being precipitated by ions formed by the electrolysis, eq. (22). Oxidation products and polymers might be produced by the radical chain reactions (15)–(17), explaining why fuels of low oxidative stability produce more deposits [22,21]. Insulation of the injector by the deposit layer [11] can lead to deposit capacitor breakdowns and a graphitization process, explaining the formation of a graphitic layer at the relatively low T of the injector.

Increased content of water in the fuel is known to increase significantly the rate of injector corrosion and injector deposit accumulation. This is in agreement with the electrokinetic mechanism, as water is known to increase the streaming current [11]. Beck et al. reported that the occurrence of water in the hydraulic liquid increases the ς-potential and causes higher current and corrosion [3]. The increased acidic content in the fuel also affects the deposition processes [6,7,49]; it can be explained with the fact that the ς-potential is a strong function of the acid concentration.

The order of magnitude of the rate of formation of the internal injector deposits can be estimated from the work of Schümann et al. [10]. They investigated needle deposits for 100, 200, 300 h injector test runs. They measured internal deposits of thickness 0.1, 0.22, and 0.25 μm respectively (at leakage temperature of 130 °C), or 0.8–1.2–2 μm (at leakage temperature of 165 °C). The diesel they investigated contained 7 % FAME. In the absence of oxygen, the internal deposits were reduced by 80 %. The reduction by 80 % can be explained with the value of the radical chain length of ν = 8: in the absence of oxygen, the oxidation is mitigated (only termination products form) but the deposition of electrolytes continues unaffected. Therefore, the moles of deposited molecules decreases from 8 + 2 to 2, see eq. (26).

3. Experimental design and results

Most elements of the mechanism in the beginning of Section 2 have already been studied to some extent: the experiments of Beck et al. and others [1,11,36,50] present detailed data for the streaming current I_s driven by a flow Q through an orifice. The high ς-potential of the steel|fuel interface is well-documented [11,36]. The earthing current I_e induced by I_s has been measured directly by Beck et al. [1,2]. The corrosive/deposit-producing nature of I_e has been demonstrated, and both metal dissolution and film deposition have been observed, depending on the value of the potential [17].

One question that remains unresolved is whether the electron transfer through the steel|fuel interface can initiate radical chain oxidation of the fuel and produce significant amount of sludge deposits. To investigate this question, we designed a test similar to the one used by Beck et al. [17]. Two electrodes were placed in an opened glass container filled with 50–80 mL diesel fuel (Fig. 2). The electrodes were made from stainless steel type 1.4307/1.4301, area 11.9 cm^2;

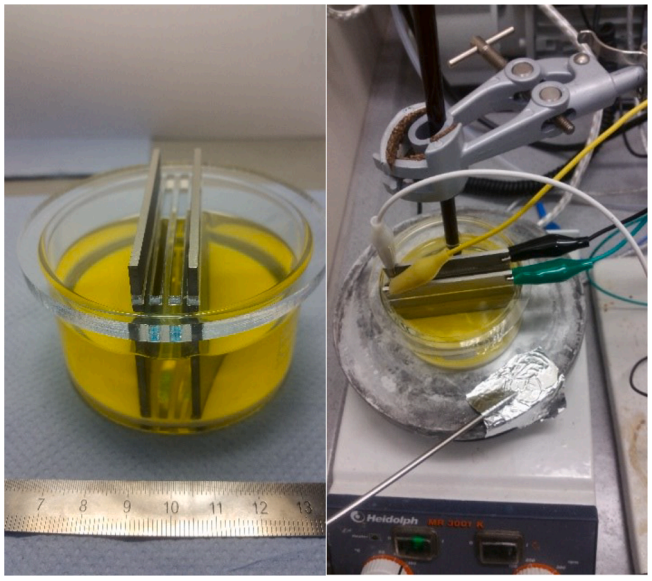

Fig. 2. Electrolysis cell used.

experiments with polished and unpolished electrodes have been performed. A commercially available fully formulated diesel fuel (European standard, specified by EN 590) was bought from a fuel station in 2018 and was used for all experiments within the next 4 months. The distance between the electrodes was varied between 1.5 and 10 mm. DC voltage of 15–30 V was applied between the electrodes. During the passage of current, the temperature was kept at 80 ± 3 °C (representative of the temperature inside an operating injector). The experiment continued for several days; for safety reasons, it was discontinued during non-working hours. During the non-working period the temperature was 20 °C when the electrodes were not under applied potential.

Four tests were performed. The first two tests were designed to choose appropriate conditions and geometry of the cell.

Test #1: small current. In test #1, the distance between the electrodes was 10 mm and 15 V potential was applied (unpolished electrodes). A current of around 0.9 μA has been measured, and it did not alter significantly for the duration of the experiment (31 h). No visible change in the fuel consistency was observed. The total charge transfer for 31 h is ∼ 0.1C, corresponding to a concentration of ∼ 0.015 mM of electrolytic degradation products at each electrode, or 0.03 mM in total.

Test #2: high current. The distance between the electrodes was decreased to 1.5 mm, and the applied voltage was increased to 30 V. Polished electrodes were used for test #2. The initial current was 3.1 μA, and it decreased steadily with time. The static resistance as estimated from the impedance spectra increased from an initial value 45 G Ω cm^2, to 65 G Ω cm^2 after 10 h, and to ∼ 400 G Ω cm^2 after 100 h. A similar drop in the current was observed by Beck et al. [17] and was related to deposition of a film onto the electrodes. The total charge transfer for 160 h is ∼ 2 C, corresponding to ∼ 0.6 mM of electrolytic degradation products (and perhaps $(1+\nu)\times 0.6 \sim 3$ mM of oxidation products). If all degradation products precipitate on the electrodes, a film of the order of 0.5 μm would form.

After 160 h, a sudden phase separation of the fuel occurred, with a thick, sticky, dark-coloured liquid separating as droplets (Fig. 3). The colour of the fuel phase itself was visibly darker than the unperturbed diesel. Both the colour change and the phase separation are typical for autooxidation. The amount of gum and sludge is visibly very high (we estimate the volume of the droplets found in a 20 mL fuel probe at 500 μL, corresponding to oxigenates concentration of around two orders of magnitude higher than the value 3 mM expected from the electrokinetic mechanism).

With the next two tests, the source of the degradation was investigated.

Test #3 and #4: high current vs no current. In test #3, the distance between the electrodes was set to 2.3 mm, and the applied voltage was 30 V. Unpolished electrodes were used. Results were similar to test #2, and phase separation took place after ∼ 160 h at 30 V and 80 °C.

The blank probe Test #4 was run in parallel with test #3, with no applied potential between the electrodes while all other conditions were kept the same (unpolished electrodes, equivalent temperature programme). The result was again similar – even in the absence of current, the diesel fuel degraded visibly and phase separated after about 160 h. This suggest that the oxidative degradation in tests #2 and #3 is not due to autooxidation initiated by the electrochemical processes at the steel|fuel interface; the increased temperature alone is enough to produce the observed level of autooxidation.

For tests #3 and #4, the specific resistivity of the fuel was followed as function of time (Fig. 4). This was done via impedance measurements before and after each non-working period, and a few measurements in an open-circuit voltage (OCV) cell. For the first 100 h of the degradation, the apparent resistivity of the cell increased steadily, by an order of magnitude. This is probably due to film formation at the electrode surface. From 100 to 160 h, the resistivity quickly decreases, due to the significant oxidation of the fuel. The 100 h induction period for the oxidation is probably due to the presence of anti-oxidant in the diesel

Fig. 3. The fuel after 160 h at 30 V, 80 °C.

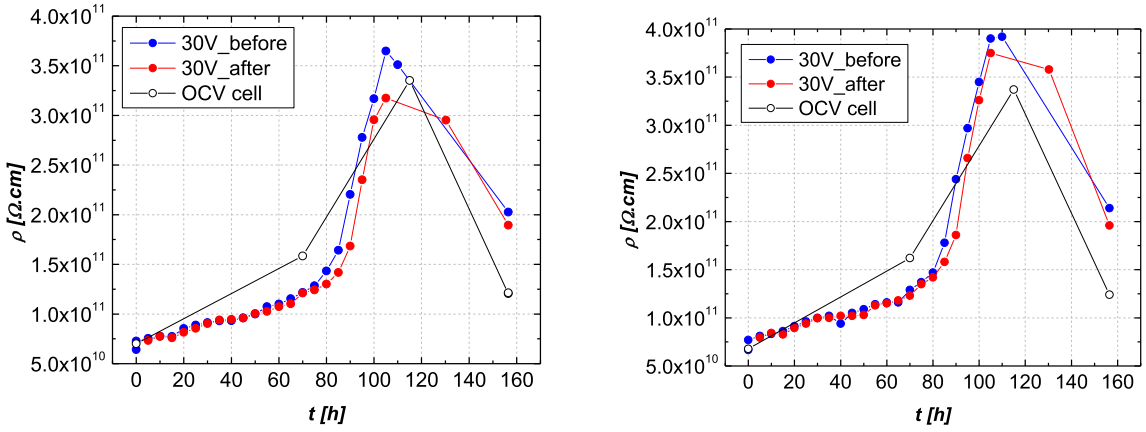

Fig. 4. Specific resistance ρ [Ω•cm] of the cell obtained from electrochemical impedance spectroscopy (left) and from measurements at constant voltages (right) vs time t [h]. The resistance was measured before and after each non-working period (impedance) and in OCV cell.

(the oxidation accelerates after the anti-oxidant is exhausted). The difference between the apparent resistivity of the cell in test#3 (30 V) and the blank test#4 is small: it appears that the zero probe degrades faster, which we ascribe to the slightly higher temperature.

4. Conclusions

In this work, a hypothesis has been formulated and tested: that the internal injector deposits in diesel engines are formed due to conjugated streaming and earthing currents. We extended the electrokinetic erosion mechanism for flows through restrictions of Beck et al. [1] to deposit formation inside fuel injectors. The analysis of this mechanism (Section 2) shows that for each excess charge carried through the orifice, one charge crosses the metal|fuel interface to produce one precipitation event like (22) at each electrode. The charge transfer through the interface also initiates a radical chain of expected length of about $\nu =$ 3–15, which produces $1 + \nu$ oxidized molecules in the fuel. Based on these conclusions, the amount of deposits can be readily computed from the value of the streaming current; the streaming current itself can be estimated from the conductivity of the fuel and the ς-potential of steel|oil, eq. (7) and (9). The expected chemistry of the electrokinetic deposits is at least in broad agreement with that of field injector deposits.

The hypothesis has been tested using an electrode cell steel|diesel|steel, where the diesel is kept at 80 °C. The main result from the test is negative: under the investigated conditions, the direct oxidation of the diesel produces more sludge than the electrokinetic mechanism, by 1–3 orders of magnitude, judging by the volume of the phase-separated material. With and without current, phase separation of the oxidized products takes place after ~ 160 h at 80 °C. The deposits formed at the metal surface are of approximately similar amount, judging from their effect on the apparent resistivity of the cell (Fig. 4). Thus, even if the electrokinetic mechanism contributes to the deposition, in the test rig, the main effect is different. It is an open question whether the oxidation process can produce the same amount of deposits in an operating injector, where the fuel is constantly exchanged. It also remains unclear if the electric current changes the chemical nature of the deposit produced by the bulk oxidation process.

Declaration of Competing Interest

The authors declare the following financial interests/personal relationships which may be considered as potential competing interests: The authors report financial support was provided by bp-ICAM. For the purpose of open access, the authors have applied a CC BY licence to any Author Accepted Manuscript version arising.

Data availability

No data was used for the research described in the article.

Acknowledgement

Funding and technical support from bp through the bp International Centre for Advanced Materials (bp-ICAM) made this research possible. For the purpose of open access, the author has applied a CC BY licence to any Author Accepted Manuscript version arising.

References

[1] Beck TR, Mahaffey DW, Olsen JH. Wear of small orifices by streaming current driven corrosion. Am Soc Mech Eng J Basic Eng 1970;92:782–8.
[2] Discussion: "Wear of Small Orifices by Streaming Current Driven Corrosion" (Beck, T. R., Mahaffey, D. W., and Olsen, J. H., 1970, ASME J. Basic Eng., 92, pp. 782–788) *Am. Soc. Mech. Eng. J. Basic Eng.* **92** (1970) 789-791.
[3] Beck TR. Electrokinetic-current corrosion. J. Electrochem. Soc. 2006;153:B181–6.
[4] Stoeck T, Osipowicz T, Abramek KF. Methodology for the repair of DENSO common rail solenoid injectors. Maintenance and Reliability 2014;16:270–5.
[5] de Macêdo Neto JC, de Oliveira MAB, del Campo ERB, da Cruz RWA, do Nascimento NR, Neto JE. Failure in fuel nozzles used in diesel engines. J. Mech. Eng. Automation 2015;5:237–40.
[6] Tanaka A, Yamada K, Omori T, Bunne S, Hosokawa K. Inner diesel injector deposit formation mechanism. SAE 2013. 2013-01-2661.
[7] Richter B, Crusius S, Schuman U, Harndorf H. Characterisation of deposits in common-rail injectors. MTZ 2013;74:50–6.
[8] J. Barker and J. Reid. Injector and fuel system deposits. Paper from 10th International Colloquium Fuels Conventional and Future Energy for automobiles (2015).
[9] Stepien Z. Types of internal diesel injector deposits and counteracting their formation. Combustion Engines 2015;163:79–91.
[10] U. Schümann, C. Fink, R. Junk, S. Crusius, and B. Buchholz. Fuel-related deposits in common-rail injectors. *SAE* (2016) Fuel system deposits, formation and effects workshop, Baltimore (24-26 Oct 2016).
[11] Klinkenberg A, van der Minne JL. Electrostatics in the Petroleum industry. Amsterdam: Cahp CI, Elsevier; 1958.
[12] Davies JT, Rideal EK. Interfacial phenomena. 2nd ed. New York and London: Academic Press; 1963. p. 122–5.
[13] Beck TR. Wear by generation of electrokinetic streaming currents. ASLE Trans 1983;26:144–50.
[14] Scenini F, Palumbo G, Stevens N, Cook A, Banks A. Investigation of the role of electrokinetic effects in corrosion deposit formation. Corros Sci 2014;87:71–9.
[15] McGrady J, Scenini F, Duff J, Stevens N, Cassineri S, Curioni M, et al. Investigation into the effect of water chemistry on corrosion product formation in areas of accelerated flow. J Nuclear Materials 2017;493:271–9.
[16] I.S. Woolsey, D.M. Thomas, K. Garbett, and G.J. Bignold. Occurrence and prevention of enhanced oxide deposition in boiler flow control orifices. In: Water chemistry of nuclear reactor systems 5, proceedings of the fifth international conference, 1989. https://doi.org/10.1680/wconrs5v1.15470.0033.
[17] Beck JR, Mahaffey DW, Olsen JH. Pitting and deposits with an organic fluid by electrolysis and by fluid flow. J Electrochem Soc 1972;119:155–60.
[18] Varga IK, Dunne LJ. Streaming potential cells for the study of erosion-corrosion caused by liquid flow. J Phys D 1985;18:211–20.

[19] Touchard GG, Romat H. Electrostatic charges convected by flow of a dielectric liquid through pipes of different length and different radii. J Electrost 1981;10:275–81.

[20] Chen H, Touchard GG, Radke CJ. A linearized corrosion double-layer model for laminar flow electrification of hydrocarbon liquids in metal pipes. Ind Eng Chem Res 1996;35:3195–202.

[21] Stepien Z. The reasons and adverse effect of internal diesel injector deposits formation. Combustion Engines 2014;156:20–9.

[22] Urzedowska W, Stepien Z. Prediction of threats caused by high FAME diesel fuel blend stability for engine injector operation. Fuel Proc Technol 2016;142:403–10.

[23] Denisov ET, Afanas'ev IB. Oxidation and antioxidants in organic chemistry and biology. CRC Taylor & Francis; 2005.

[24] Slavchov RI, Mosbach S, Kraft M, Pearson R, Filip S. An adsorption-precipitation model for the formation of injector external deposits in internal combustion engines. Appl Energy 2018;228:1423–38.

[25] A. Klinkenberg. Production of static electricity by movement of fluids within electrically grounded equipment. Proceedings of the 4th world petroleum congress, Carlo Colombo, Rome, Sec. VII/C, paper 5 (1955) 253-264.

[26] Leonard JT. Static electricity in hydrocarbon liquids and fuels. J Electrostatics 1981;10:17–30.

[27] A. J. Rutgers, M. de Smet, and G. de Myer (or de Moyer). Influence of turbulence upon electrokinetic phenomena. Experimental determination of the thickness of the diffuse part of the double layer. *Trans. Faraday Soc.* **53** (1957) 393-396; cf. also *Experentia* **12** (1956) 371.

[28] W. F. Cooper. The electrification of fluids in motion. Static electrification, a symposium held by the institute of physics in London (25-27 March 1953). *British J. Appl. Physics* **4** (1953) S11-15.

[29] Rutgers AJ, De Smet M, Rigole W. Streaming currents with nonaqueous solutions. J Colloid Sci 1959;14:330–7.

[30] Touchard G. Flow electrification of liquids. J Electrostatics 2001;51–52:440–7.

[31] Frenkel JJ. On frictional electrization. J Physics (Acad Sci USSR) 1941;14:172.

[32] Active Standard ASTM D4865, https://compass.astm.org/resolve/EDIT/?D4865+09(2014), accessed in July 2020.

[33] Gonzalez Prieto LE, Sorichetti PA, Romano SD. Electric properties of biodiesel in the range from 20 Hz to 20 MHz. Comparison with diesel fossil fuel. Int J Hydrogen Energy 2008;33:3531–7.

[34] Minkov IL, Arabadzhieva D, Salama IE, Mileva E, Slavchov RI. Barrier kinetics of adsorption-desorption of alcohol monolayers on water under constant surface tension. Soft Matter 2019;15:1730–46.

[35] Merritt HE. Hydraulic control systems. NY: Wiley & Sons; 1967.

[36] Paillat T, Cabaleiro JM, Romat H, Touchard G. Flow electrification process: the physicochemical corroding model revisited. IEEE Trans Dielectrics Electrical Insulation 2009;16:359.

[37] B.B. Damaskin, O.A. Petriy, and G.A. Tzirlina. Electrochemistry. Chemistry, Moscow, 2001 (in Russian). Sec. 6.4. Classification of electrodes.

[38] Vijh AK, Conway BE. Electrode Kinetic Aspects of the Kolbe Reaction. Chem Rev 1967;67:623–64.

[39] T. Shono, Y. Matsumura, and K. Tsubata. Anodic oxidation of *N*-carbomethoxypyrrolidine: 2-methoxy-*N*-carbomethoxypyrrolidine. *Organic Syntheses*, Coll. Vol. 7, p.307 (1990); Vol. 63, p.206 (1985). DOI:10.15227/orgsyn.063.0206.

[40] Jones AM, Banks CE. The Shono-type electroorganic oxidation of unfunctionalized amides. Carbon-carbon bond formation via electrogenerated N-acyliminium ions. Beilstein J Org Chem 2014;10:3056–72.

[41] Srivastava SP, Hancsóc J. Fuel and fuel-additives. Hoboken, New Jersey: Wiley; 2014.

[42] Kapustin VM. Petroleum and alternative fuels with additives and dopants. Moscow: KolosS; 2008. In Russian.

[43] Ohya-Nishiguchi H. Both oxidation and reduction of aromatic hydrocarbons by an electrolysis cell design for low-temperature ESR studies. Bull Chem Soc Japan 1979;52:2064–8.

[44] Bamford CH, Tipper CFH, editors. Comprehensive Chemical Kinetics. Amsterdam, Netherlands: Liquid-Phase Oxidation. Elsevier; 1980.

[45] J. Barker, C. Snape, and D. Scurr. A novel technique for investigating the characteristics and history of deposits formed within high pressure fuel injection equipment. *SAE Int. J. Fuels Lubr.* 5 (2012) 1155-1164/SAE 2012-01-1685.

[46] J. Ullmann, M. Geduldig, H. Stutzenberger, R. Caprotti, and G. Balfour. Investigation into the formation and prevention of internal diesel injector deposits. *SAE Technical Paper* 2008-01-0926.

[47] J. Barker, C. Snape, and D. Scurr. Information on the aromatic structure of internal diesel injector deposits from time of flight secondary ion mass spectrometry (ToF-SIMS). *SAE Technical paper* 2014-01-1387.

[48] Lau K, Junk R, Klingbeil S, Schümann U, Streibel T. Analysis of internal common rail injector deposits via thermodesorption photon ionization time of flight mass spectrometry. Energy Fuels 2015;29:5625–32.

[49] Reid J, Cook S, Barker J. Internal injector deposits from sodium sources. SAE Int J Fuels Lubr 2014;7. SAE 2014–01-1388.

[50] Kelly DN, Lam RK, Duffin AM, Saykally RJ. Exploring Solid/Aqueous Interfaces with Ultradilute Electrokinetic Analysis of Liquid Microjets. J Phys Chem C 2013;117:12702–6.